Al$_2$O$_3$:　　　　　Pt/Al$_2$O$_3$

1　　　　　*,1,2

(　　　　　　　，　　201418)

(　　　　　　　　　　，　　200237)

：“　　　　（EA）－　　　－　　”　　　　　　　　　Al$_2$O$_3$。　　　：　　　　　　、

、NaAlO$_2$　　、EA　　　　　　　　　　　　；，　　　　γ-Al$_2$O$_3$　　　Pt/γ-Al$_2$O$_3$　　　　，

　　Al$_2$O$_3$　　Pt/Al$_2$O$_3$　　　　　　　PtO$_x$　　。　　　　　　　，　　Al$_2$O$_3$

Pt/Al$_2$O$_3$　　，　　　γ-Al$_2$O$_3$　　Pt/γ-Al$_2$O$_3$　　　　。

：　　　；　　；　　；Pt/Al$_2$O$_3$

：O614.3$^+$1　　　　　：A　　　　：1001-4861(2011)10-2045-08

Mesoporous Al$_2$O$_3$ Assembled by Nano-Films: Synthesis and Pt/Al$_2$O$_3$ Performance for Catalytic Hydrogenation of Nitrobenzene

LIU Hui-Ping[1]　　LU Guan-Zhong[*,1,2]

(*Shanghai Institute of Technology, Shanghai 201418, China*)
(*Lab for Advanced Materials, Research Institute of Industrial Catalysis, East China University of Science and Technology, Shanghai 200237, China*)

Abstract: In the synthesis solution of "Ethyl Acetate (EA)-NaAlO$_2$-H$_2$O", the nano-films assembled mesoporous Al$_2$O$_3$ was synthesized at room temperature. The morphology of the synthesized Al$_2$O$_3$ are affected by the reaction time, aging time under stirring before standing, NaAlO$_2$ and EA amounts, and reaction temperature. Using synthesized Al$_2$O$_3$ and commercial γ-Al$_2$O$_3$ as the support, the Pt catalysts were prepared by an incipient wetness impregnation method. Compared with Pt/γ-Al$_2$O$_3$, Pt/Al$_2$O$_3$ catalyst prepared with nano-films assembled mesoporous Al$_2$O$_3$ has some PtO$_x$ species that can be reduced more easily. In the catalytic hydrogenation of nitrobenzene, Pt/Al$_2$O$_3$ has higher catalytic activity than that of Pt/γ-Al$_2$O$_3$.

Key words: mesoporous material; nano particles; hydrogenation; Pt/Al$_2$O$_3$

Al$_2$O$_3$ is an important basic chemical raw material, and has been used widely in industrial catalysts, supports, and other fields for its special propetites such as the high thermal, chemical and mechanical stabilities, structural characteristics and lower price [1-4]. Since the ordered mesoporous SiO$_2$ has been discovered [5], many strategies have been used to study the mesoporous Al$_2$O$_3$. Over the past twenty years, varied kinds of mesoporous Al$_2$O$_3$ have been obtained [6-11]. The textural and porous properties of Al$_2$O$_3$, such as surface area, pore size distribution and pore volume, are important for Al$_2$O$_3$ application because of their direct relations with the catalytic performances [12-13]. In addition, the morphology of Al$_2$O$_3$ also has great effect on its property

and application, for example, nano-fibrous Al_2O_3 with random stacking and low contact area exhibits a strong resistance to sintering [14]. Though the structure and morphology control is very important, there are very limited studies on the structurally and morphologically synthesis of mesoporous Al_2O_3 [15-16]. To the best of our knowledge, there has been no report available on mesoporous Al_2O_3 assembled by curved nano-films, although Al_2O_3 has been investigated and used for many years.

Here we report a simple procedure for the synthesis of a mesoporous Al_2O_3 particles assembled by curved nano-films. The procedure consists of gradual addition of Ethyl Acetate (EA) into $NaAlO_2$ solution under magnetic stirring and a few hours standing for precipitation. After thermal treatment, porous Al_2O_3 particles assembled by curved nano-films were obtained.

In order to show the performance of the sample synthesized, Pt/Al_2O_3 was prepared by the incipient wetness impregnation method, and then was used for the nitrobenzene (NB) hydrogenation reaction. For comparison, Pt/γ-Al_2O_3 was also prepared with the commercial γ-Al_2O_3 powder by the same way and used in the NB hydrogenation reaction.

1 Experimental

1.1 Reagents

$NaAlO_2$ (A.R.) was purchased from Shanghai Lingfeng Chemical Reagent Co., Ltd.. Ethyl acetate (EA) (A.R.), ethanol. (A.R.), nitrobenzene (NB, A.R.) and $H_2PtCl_6 \cdot 6H_2O$ (A.R.) were purchased from Sinopharm Chemical Reagent Co., Ltd., Shanghai.

1.2 Synthesis

Preparation of Al_2O_3: 0.52 g $NaAlO_2$ was dissolved in 150 mL deionized water at 25 ℃, then 2 g of EA was added dropwise into the above $NaAlO_2$ solution under magnetic stirring. After being stirred for about 1 min, the mixture was kept at 25 ℃ for 10 h. The formed white precipitate was separated, washed, dried, and then calcined at 550 ℃ for 5 h or at 1 000 ℃ for 24 h.

Preparation of the Pt-containing catalysts: Pt/Al_2O_3 was prepared by the incipient wetness impregnation

method using Al_2O_3 calcined at 550 ℃ as the support and H_2PtCl_6 aqueous solution as Pt source. After drying, the catalyst was calcined at 550 ℃ for 5 h for later investigation. Pt/γ-Al_2O_3 was prepared with commercial γ-Al_2O_3 powder (purchased from BASF) by the same process. And Pt loading for both catalysts was 5.0wt%.

1.3 Characterization

The scanning electron micrograph (SEM) of the sample was obtained on a JSM-6360LV scanning microscope operated at an accelerating voltage of 15 kV. The transmission electron microscope (TEM) images were obtained on a Philips CM200 FEG\ST Lorentz electron microscope with a field emission gun at an acceleration voltage of 200 kV. N_2 sorption isotherm of the sample was obtained at 77 K on an automated physisorption instrument (NOVA 4200e, Quantachrome Instruments). The specific surface area was calculated by the Brunauer-Emmett-Teller(BET) method and the pore size distribution was obtained by the Barret-Joyner-Halenda (BJH) method from the desorption data. The hydrogen temperature-programmed reduction (H_2-TPR) was performed in a quartz reactor under 5 vol.% H_2/N_2 flow (30 mL·min^{-1}) from 30 to 550 ℃ at a heating rate of 10 ℃·min^{-1}. A thermal conductivity detector (TCD) was used to follow the H_2 consumption. A PM5A column was used to trap the water formed during the process. The Pt dispersion of the catalysts was determined by the method reported in our previous work[12], it was determined by a pulse titration of H_2-O_2 on an AUTOSORB-6B pulse chemisorption analyzer (Quantachrome), and a PM5A column was used to trap water formed during the testing process. At first, 100 mg catalyst was reduced in situ in H_2 flow of 30 mL·min^{-1} at 350 ℃ for 3 h, and then was swept with Ar flow of 50 mL·min^{-1} for 3 h and the temperature of reactor fell to 25 ℃. Then this reduced catalyst was treated with O_2 flow of 30 mL·min^{-1} for 1 h, followed by sweeping with Ar flow of 50 mL·min^{-1} for 1 h. After that, the H_2 pulses were injected with the mixture gas of 5% H_2 in Ar by a calibrated on-line sampling value, in which the mixture gases of 5% H_2 in Ar were catalytically purified over the oxidized catalyst. The H_2 adsorption was assumed to be completed after five

successive peaks with the same peak area. The H$_2$ uptake measured was used to estimate the Pt dispersion.

1.4 Catalytic testing

Catalytic hydrogenation of NB was performed in a 150 mL stainless-steel autoclave equipped with a magnetic stirrer in a thermostated water bath. After being reduced in H$_2$, 0.05 g catalyst was transferred into the autoclave, and then 25 mL ethanol and 0.6 g NB were added. The reaction was kept stirring at room temperature for 10 min under 0.5 MPa pressure of H$_2$. The products were analyzed by gas chromatograph (GC, PerkinElmer Clarus 500) equipped with an FID detector and a CHIRALSIL-DEX × CB silica capillary column (25 m×0.25 mm×0.25 μm). The injection and column temperature was 180 ℃. The detector temperature was 220 ℃. The carrier gas was N$_2$ with a flow rate of 0.7 mL· min^{-1} in a split ratio of 1:40. The intermediates produced during the reaction process were determined by GC-MS (HP6890-Micromass GCTTM) equipped with HP-35MS silica capillary column (30 m×0.25 mm×0.25 μm). He was used as the carrier gas at a constant flow rate of 1.0 mL·min^{-1}, with a split ratio of 1:50. The injection port and column temperature was 200 ℃ , 240 ℃ ,

respectively. The ionization source was maintained at 280 ℃. Ionization was done by electron impact ionization (EI) at 70 eV. The mass scan range was set to 5~200 m/z. The solvent delay time was 3 min.

2 Results and discussion

2.1 Physicochemical properties of Al$_2$O$_3$ assembled by nano-films

SEM images of the synthesized Al$_2$O$_3$ is presented in Fig.1a, in which the left reveals that the synthesized Al$_2$O$_3$ is composed of irregular particles connected with each other. The enlarged image (the right of Fig.1a) shows that Al$_2$O$_3$ particles look like being composed of a great number of curved nanofibers with an average diameter of 40 nm. However, TEM image presented in Fig.1b reveals that the synthesized Al$_2$O$_3$ particle is composed of many cross-linked nano-films, indicating the nanofibers observed from the SEM images are actually the edges of these nano-films. Besides, Fig.1b also reveals that the Al$_2$O$_3$ particle has a hollow structure. These Al$_2$O$_3$ particles are interconnected with each other by the cross-linked nano-films, which makes them hard to be separated into individual particle, see Fig.1c.
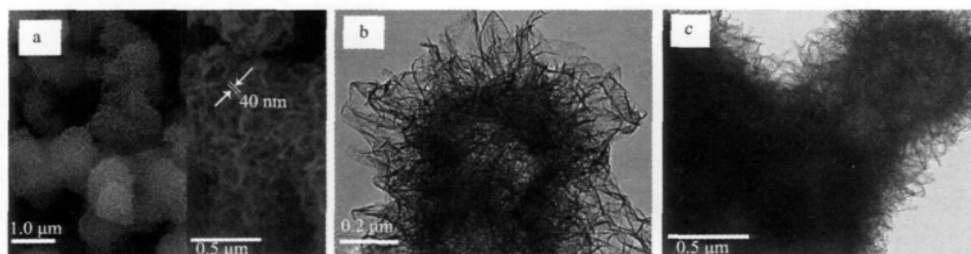

Fig.1 (a) SEM and (b, c) TEM images for the synthesized Al$_2$O$_3$

N$_2$ adsorption/desorption isotherm of the synthesized Al$_2$O$_3$ (Fig.2) shows a type-IV (IUPAC[17]) curves with a H3 desorption hysteresis loop in $P/P_0=$ 0.6~1.0, indicating an existence of non-uniform slit-like mesopores in the sample. The pore size distribution of Al$_2$O$_3$ is broad and mainly ranges from 6 to 20 nm but a few ranges from 20 to 100 nm (inset in Fig.2). The BET surface area and pore volume of Al$_2$O$_3$ calcined at 550 ℃ for 5 h are 265 m^2·g^{-1} and 0.74 cm^3·g^{-1}. It is interesting that the BET surface area of Al$_2$O$_3$ is still 68 m^2·g^{-1} even after it was calcined at 1 000 ℃ for 24 h, indicating the synthesized Al$_2$O$_3$ has good thermal
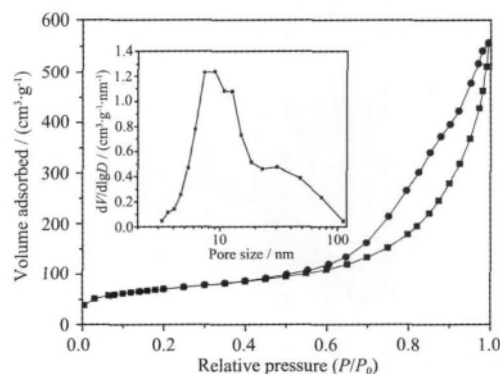
Inset: Pore size distribution for Al$_2$O$_3$ from this work

Fig.2 N$_2$ adsorption/desorption isotherms

stability, which is possibly due to its special nano-film basic structure and stacking mode[14]. In addition, this synthesized Al_2O_3 has low tap density (0.13 g·mL^{-1}) and high water adsorption capacity (830%).

2.2 Effect of reaction time

The effect of reaction time on morphology and particle size of the synthesized Al_2O_3 is shown in Fig.3. When the synthesis solution is kept standing at 25 ℃ for 1 h, the obtained Al_2O_3 particles are irregular spherules with diameters less than 250 nm (Fig.3a), and the TEM image (inset in Fig.3a) reveals that the Al_2O_3 spherules are composed of nano-films. Furthermore, there are only a small amount of product, meaning the uncompleted hydrolysis reaction of $NaAlO_2$. When the reaction time is extended to 5 h, the synthesized Al_2O_3 particles become bigger and are composed of the curved nano-films intersected with each other (Fig.3b). As the reaction time is extended further to 10 h or 20 h, no changes for nano-film construction unit and particle size of Al_2O_3 are visible (Fig.3c, d), but there is an increase in the amount of obtained products till maximum value is reached, indicating the completion of hydrolysis reaction for $NaAlO_2$.
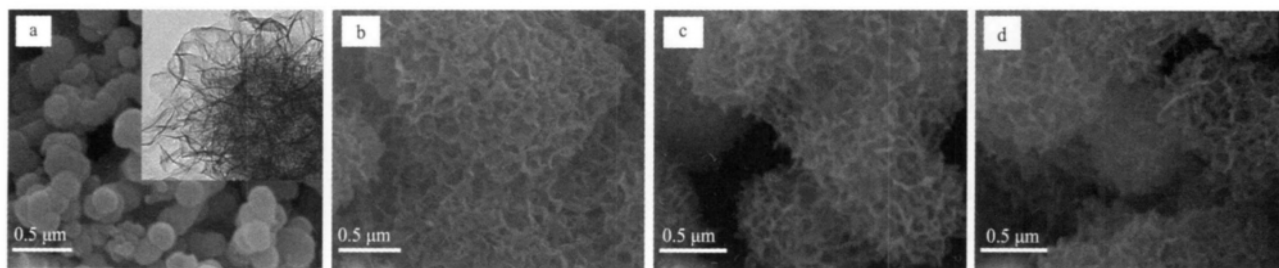

Fig.3　SEM images for Al_2O_3 synthesized for (a) 1 h, (b) 5 h, (c) 10 h and (d) 20 h

2.3 Effect of reaction temperature

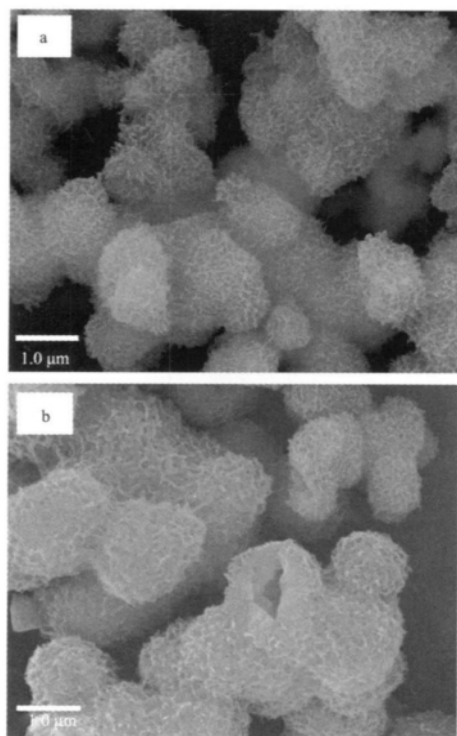Fig.4 is the SEM images of Al_2O_3 synthesized at different reaction temperatures. It reveals that the Al_2O_3 particles synthesized at 25 and 50 ℃ are similar, and they are all composed of the curved nano-films intersected with each other (Fig.4a, b). In addition, one crushed Al_2O_3 particle in Fig.4b clearly shows that it has a hollow structure. Furthermore, the results show that the amount of Al_2O_3 synthesized at 50 ℃ is obviously fewer than that of Al_2O_3 synthesized at 25 ℃. The hydrolysis process is endothermic and the elevated temperature can promote the extent of hydrolysis, resulting in more hydrolysates. However, this theoretical conclusion is in contradiction with the experimental result that the amount of Al_2O_3 synthesized at 50 ℃ is fewer than that of Al_2O_3 synthesized at 25 ℃. The possible cause may be that the initially formed $Al_m(OH)_n$ nano-films (Scheme 1) are dissolved partially in the solution at higher temperature. This can be further confirmed by no precipitate at the synthesis temperature of 80 ℃.

2.4 Effect of stirring time before standing

Effect of stirring time before standing on Al_2O_3 is shown in Fig.5. We can see that there is no obvious difference between the Al_2O_3 particles synthesized with 10 min of stirring (Fig.5a) and those synthesized using 1
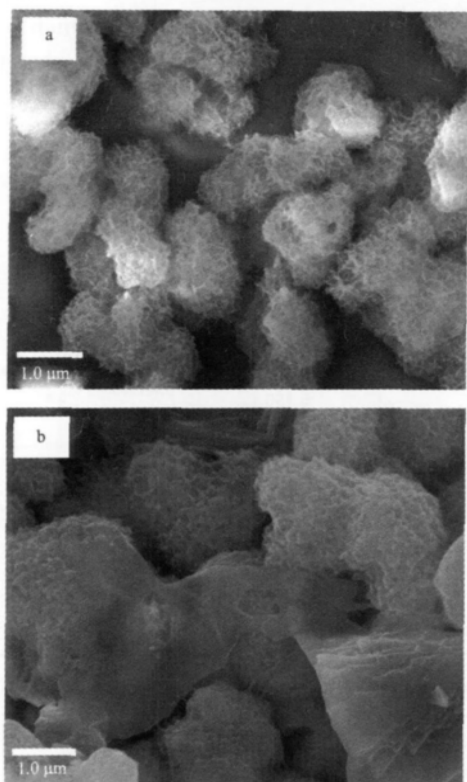

Fig.4　SEM images for Al_2O_3 synthesized at (a) 25 ℃ and (b) 50 ℃

Fig.5　SEM images for Al$_2$O$_3$ synthesized with (a) 10 min and (b) 30 min of stirring time before standing

min of stirring (Fig.1), both samples are composed of nano-films. But when the stirring time is extended further, the morphology of Al$_2$O$_3$ changes a lot. For example, when the stirring time before standing is extended to 30 min, some of the obtained Al$_2$O$_3$ particles are composed of disordered masses (Fig.5b). The reason may be that the initial formed Al$_m$(OH)$_n$ nano-films (Scheme 1) cannot deposit regularly during a too long time of stirring, but deposit as the irregular masses.

2.5　Effect of NaAlO$_2$ amount

Fig.6 reveals that NaAlO$_2$ amount has no effect on the nano-film structure of the synthesized Al$_2$O$_3$, but can affect the particle size of the sample. For example, when NaAlO$_2$ amount is 0.13 g or 0.26 g, the obtained Al$_2$O$_3$ particles are composed of the nano-films (Fig.6a, b), but the sizes of particles are obvious smaller than those of Al$_2$O$_3$ particles synthesized using 0.52 g or 0.65 g NaAlO$_2$ (Fig.6c,d). In addition, from the results we find that the yield of Al$_2$O$_3$ increases with increasing NaAlO$_2$ amount within the range investigated.
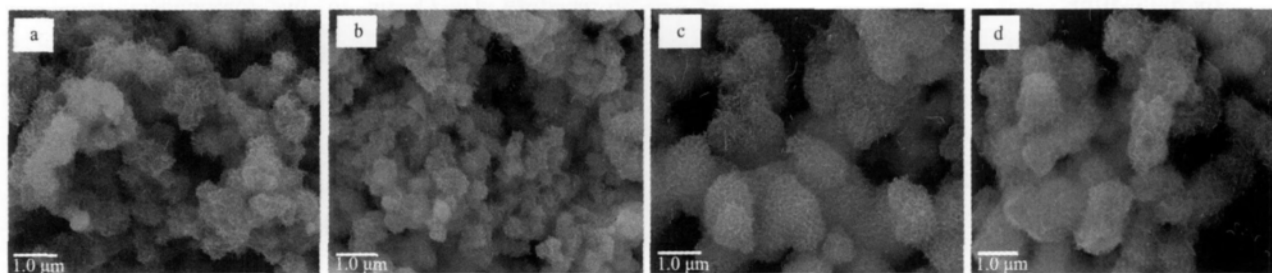

Fig.6　SEM images of Al$_2$O$_3$ synthesized with (a) 0.13 g, (b) 0.26 g, (c) 0.52 g and (d) 0.65 g NaAlO$_2$

2.6　Effect of EA amount

Fig.7 shows SEM images for Al$_2$O$_3$ synthesized with (a) 1.0 g, (b) 2.0 g and (c) 3.0 g EA. From Fig.7, one can see that EA amount within the range investigated has no obvious effect on the morphology of the synthesize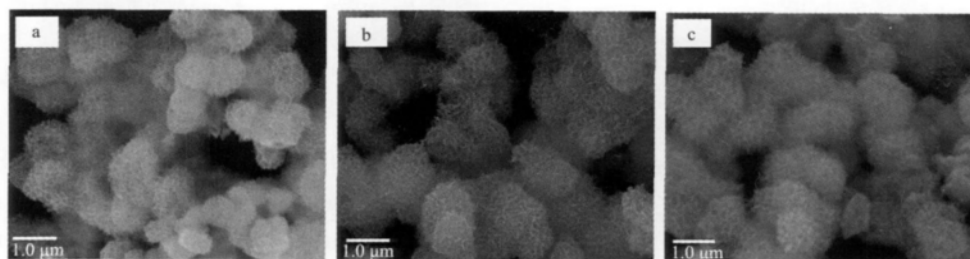d products. However, our observation on the turbid time does indicate that increase in EA amount can shorten the turbid time of the reaction solution, indicating that increasing EA amount in the synthesis solution may accelerate the hydrolysis of NaAlO$_2$, and consequently, the precipitate is formed in a relatively short time.

Fig.7　SEM images for Al$_2$O$_3$ synthesized with (a) 1.0 g, (b) 2.0 g and (c) 3.0 g EA

Additionally, N$_2$ adsorption/desorption isotherms and the pore size distribution of the synthesized Al$_2$O$_3$ indicate that EA amount in the synthesis solution has effect on the BET surface area, pore size distribution

and pore volume of the obtained Al$_2$O$_3$, which increase with increasing of EA in the synthesis system within the range investigated (Fig.8 and Table 1).
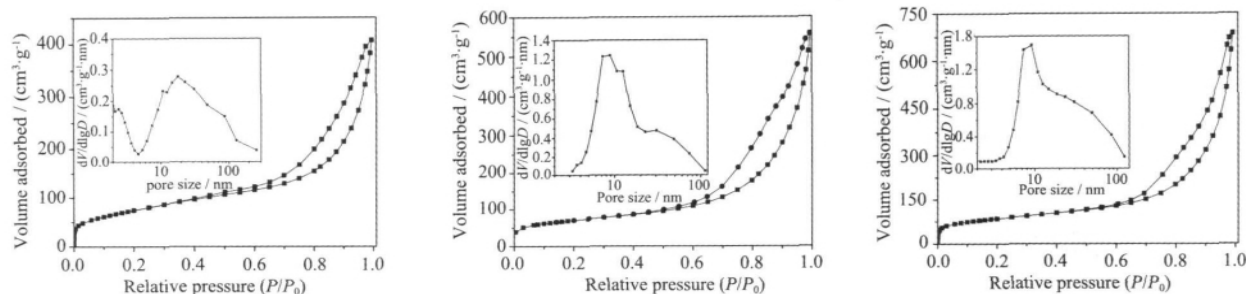

Fig.8　N$_2$ adsorption/desorption isotherms(Inset: Pore size distribution) for Al$_2$O$_3$ synthesized with (a) 1.0 g, (b) 2.0 g and (c) 3.0 g EA

Table 1　Textural properties of Al$_2$O$_3$ measured by N$_2$ physisorption

Sample	Amount of E_A / g	D_{BJH} / nm	S_{BET} / (m$^2 \cdot$g^{-1})	V_t / (cm$^3 \cdot$g^{-1})
Al$_2$O$_3$	1.0	8.6	251	0.59
Al$_2$O$_3$	2.0	12.7	265	0.74
Al$_2$O$_3$	3.0	13.4	292	0.98

2.7　Formation process of Al$_2$O$_3$ particles assembled by nano-films

A possible formation process of Al$_2$O$_3$ particles assembled by nano-films is proposed as Scheme 1 based on experimental results. When NaAlO$_2$ is dissolved in water at room temperature, the hydrolysis procedure 1 will occur, but the precipitate can not be formed because of low degree hydrolysis; when EA is added dropwise in the above solution, hydrolysis procedure 2 occurs, simultaneouly, reaction 3 takes

place, which promots the hydrolysis of NaAlO$_2$ (procedure 1). Owing to the low concentration of NaAlO$_2$ and EA in the reaction solution, hydrolysis of NaAlO$_2$ and EA takes place very slowly and promots each other simultaneously. During these processes, Al(OH)$_3$ aggregations are formed and further grow into the Al$_m$(OH)$_n$ nano-films, which then are cross-linked each other and self-assembled into microparticles with a hollow structure (procedure 4 and 5).
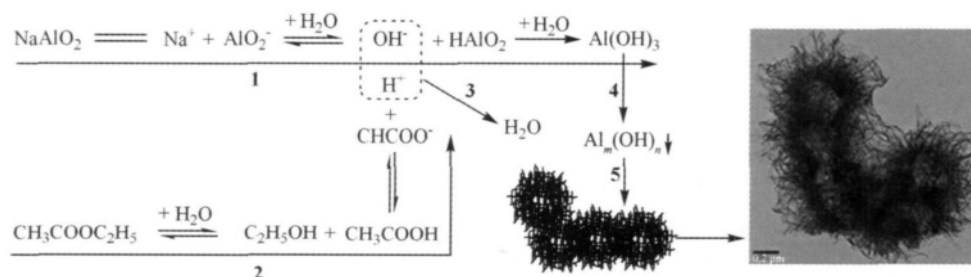
Scheme 1　Possible formation processes of Al$_2$O$_3$ particles assembled by nano-films

2.8　Catalytic performance of Pt/Al$_2$O$_3$ for NB hydrogenation

TEM image of the calcined Pt/Al$_2$O$_3$ is presented in Fig.9a, in which the grey part indicates the Al-O

framework of Al$_2$O$_3$, and the dark dots are PtO$_x$ particles dispersed on the surface of Al$_2$O$_3$. TEM image shows that PtO$_x$ particles are very fine, though they exist as different nano-size particles and disperse randomly on
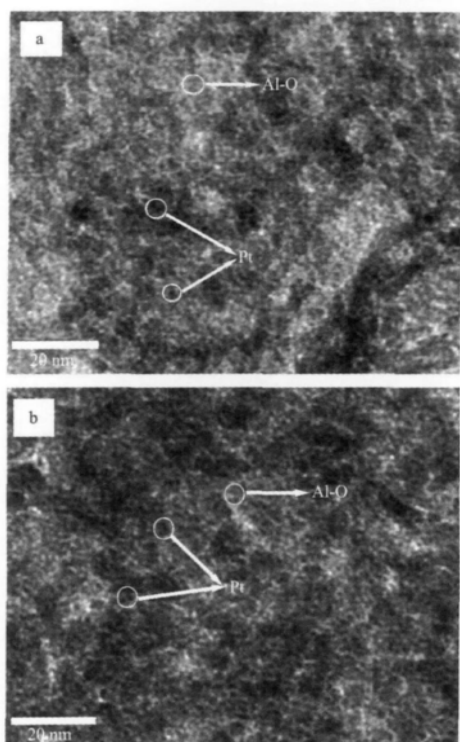
Fig.9 TEM images for (a) Pt/Al$_2$O$_3$ and (b) Pt/γ-Al$_2$O$_3$

Fig.10 H$_2$-TPR profiles for calcined (a) Pt/Al$_2$O$_3$ and (b) Pt/γ-Al$_2$O$_3$

the surface of Al$_2$O$_3$. Fig.9b shows that the supported Pt particles on γ-Al$_2$O$_3$ are also very fine and exist in the range of nano sizes. The measured Pt dispersions of Pt/Al$_2$O$_3$ and Pt/γ-Al$_2$O$_3$ are 63.3% and 61.8%, respectively.

Fig.10 shows the H$_2$-TPR profiles of the calcined Pt/Al$_2$O$_3$ and Pt/γ-Al$_2$O$_3$. Both catalysts display H$_2$ consumption peaks approximately at 170~230 ℃ and 350~430 ℃, but, for Pt/Al$_2$O$_3$, there still has a stronger reduction peak at about 80~120 ℃ and other three weaker peaks at about 155, 255 and 290 ℃. PtO$_x$ species deposited on γ-Al$_2$O$_3$ exist as two different phases[18]: (1) a dispersed phase in which PtO$_x$ particles have a strong interaction with the support, resulting in a H$_2$ consumption peak at higher reduction temperature; (2) a particulate phase in which PtO$_x$ particles are
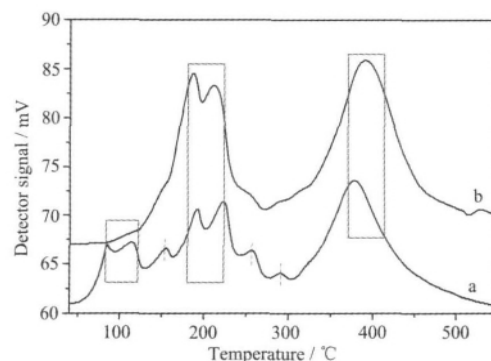
aggregated and have weak interaction with the support, resulting in a H$_2$ consumption peak at lower reduction temperature. Another cause for different H$_2$ consumption peaks at different temperatures may be owing to various positive centers, which have different interactions with PtO$_x$ particles, spreading over the framework of Al$_2$O$_3$. TEM images in Fig.9 reveal that the sizes of PtO$_x$ particles of Pt/Al$_2$O$_3$ and Pt/γ-Al$_2$O$_3$ are similar, so the different H$_2$ consumption peaks of both catalysts may be caused by the different interactions between PtO$_x$ particles and the different positive centers spreading over the framework structures of Al$_2$O$_3$ and γ-Al$_2$O$_3$.

Results of NB hydrogenation are listed in Table 2. GC-MS analysis reveals that the final product and the intermediate during the reaction process are aniline (AN) and nitrosobenzene (NSB), respectively. The results show that though the Pt dispersions of Pt/Al$_2$O$_3$ (63.3%) and Pt/γ-Al$_2$O$_3$ (61.8%) are close to each other, their catalytic activities have obvious difference. Using Pt/Al$_2$O$_3$ as the catalyst, the NB conversion is up to 99.0% in 10 min of reaction, and the selectivity to AN and intermediate NSB is 85% and 15%, respectively; while the NB conversion is only 75.7% with Pt/γ-Al$_2$O$_3$

Table 2 Catalytic performances of Pt/Al$_2$O$_3$ and Pt/γ-Al$_2$O$_3$ catalysts for the NB hydrogenation

Catalyst	Pt dispersion / %	NB conversion / %	Selectivity/%		TON[a]
			AN	NSB	
Pt/Al$_2$O$_3$	63.3	99.0	85.0	15.0	305
Pt/γ−Al$_2$O$_3$	61.8	75.7	85.7	14.3	239

[a] TON=(n_A−n_B)/n(Pt$_{surf}$), n_A and n_B denote the initial and final molar amount of NB;

n(Pt$_{surf}$) denotes the molar amount of Pt on the catalyst surface

as the catalyst, though the selectivity to AN and NSB is similar to that of Pt/Al$_2$O$_3$. Furthermore, the turnover numbers (TONs) of Pt/Al$_2$O$_3$ and Pt/γ-Al$_2$O$_3$ are 305 and 239, respectively. The different catalytic activities of Pt/Al$_2$O$_3$ and Pt/γ-Al$_2$O$_3$ may be caused by the different Pt nano-particles that have dissimilar interactions with different Al-O frameworks of Al$_2$O$_3$ and γ-Al$_2$O$_3$, and the further investigation is necessary for the elucidation of this result. Anyhow, the prepared Al$_2$O$_3$ assembled by nano-films is a good support for preparing Pt/Al$_2$O$_3$.

3   Conclusions

In summary, a facile method based on a hydrolysis-precipitation process by using NaAlO$_2$ as Al source and EA as hydrolytic accelerator was developed to synthesize Al$_2$O$_3$ particles assembled by nano-films. The BET surface of the synthesized Al$_2$O$_3$ retains 68 m$^2 \cdot$g^{-1} even after the sample is calcined at 1 000 ℃ for 24 h, which is possibly due to the special nano-structure and stacking mode of the nano-films assemblies. In the synthesis of Al$_2$O$_3$ particles assembled by nano-films, the reaction conditions such as the temperature and stirring time before standing have great effects on morphology and particle size distribution of the final products. For example, when the reaction temperature gets to 50 ℃ or the stirring time before standing lasts for 30 min, the synthesized Al$_2$O$_3$ tends to be massive shape, and if the synthesis temperature reaches 80 ℃, the solid product cannot be obtained.

In addition, the above-synthesized Al$_2$O$_3$ is a good support for preparing Pt/Al$_2$O$_3$, which has excellent catalytic activity in the hydrogenation of NB under mild reaction conditions.

References:

[1] Ttueba M, Trasatti S P. Eur. *J. Inorg. Chem.*, **2005,17**:3393-3403

[2] Breysse M, Afanasiev P, Geantet C, et al. *Catal. Today*, **2003,86**:5-16

[3] Pineda M, Palacios J M. *Appl. Catal. A*, **1997,158**:307-321

[4] Wang L, Zhang F, Chen J M. *Environ. Sci. Technol.*, **2001, 35**:2543-2547

[5] Kresge C T, Leonowicz M E, Roth W J, et al. *Nature*, **1992,359**:710-712

[6] Deng W, Toepke M W, Shanks B H. *Adv. Funct. Mater.*, **2003,13**:61- 65

[7] Kim H J, Kim T G, Kim J J, et al. *J. Phys. Chem. Solids*, **2008,69**:1521-1524

[8] Liu Q, Wang A Q, Wang X D, et al. *Chem. Mater.*, **2006,18**: 5153-5155

[9] Bhattacharyya S, Gabashvili A, Perkas N, et al. *J. Phys. Chem. C*, **2007,111**:11161-11167

[10]Park H S, Yang S H, Jun Y S, et al. *Chem. Mater.*, **2007,19**: 535-542

[11]Wakihara T, Hirasaki T, Shinoda M, et al. *Crystal Growth & Design*, **2009,9**:1260-1263

[12]Liu H P, Lu G Z, Yun G, et al. *Catal. Commun.*, **2009,10**: 1324-1329

[13]Valentini A, Carrenö N L V, Probst L F D, et al. *Micropor. Mesopor. Mater.*, **2004,68**:151-157

[14]Zhu H Y, Riches J D, Barry J C. *Chem. Mater.*, **2002,14**: 2086-2093

[15]Liu Q, Wang A, Wang X, et al. *Micropor. Mesopor. Mater.*, **2006,92**:10-21

[16]Liu H P, Lu G Z, Yun G, et al. *Cent. Eur. J. Chem.*, **2009, 7**:794-802

[17]Gregg S J, Sing K S. *Adsorption, Surface Area and Porosity.* 2*nd* Ed. New York: Academic Press, **1982**.

[18]Yao H C, Sieg M, Plummer H K. *J. Catal.*, **1979,59**:365-37